

# Chaotic system and special cases in restricted three-body problem

Jiacheng Wang<sup>1, a</sup>, Jhon Tu<sup>2</sup>, Yicheng Zhao<sup>3</sup>

<sup>1</sup>Shandong Experimental High School, Jinan, 250001, China.

<sup>2</sup>United World College of Changshu, Changshu, 215501, China.

<sup>3</sup>Fuzhou No.1 High School, Fuzhou, 350001, China.

<sup>a</sup>consttwang@gmail.com.

**Abstract:** This paper mainly analyzes the chaotic systems behind the three-body problem, establishing the relationship between initial parameters of the three stars and the degree of chaos, classifying and comparing the Lagrangian (some or famous) points with computer simulation and mathematical demonstration. Moreover, this paper also presents the analysis for the special cases of three-body systems in two-dimensional plane with stabilized patterns of every specific solution with computer simulation and theoretical demonstrations.

**Keywords:** Chaotic system, Lagrangian points, Specific solution, Two-dimensional restricted, Three-body problem

## 1. Introduction

In the field of astrophysics, the three-body problem has been mysterious and debatable, with a lost of a general analytic solution for centuries. The fundamental reason for the insolubility of three-body problem is its inclusion of chaotic system, as a specific case of the n-body problem. Unlike two-body problems, no general closed-form solution exists due to the chaos of the resulting dynamical system for most initial conditions for the three stars, and numerical methods are generally required.

This work focuses on the factors that lead to the chaotic systems and the computer simulation along with mathematical analysis about our finding of special cases in two-dimensional three-body problem. It connects three-body problem with the computer simulation. The first version of the code helps to get the value of stars' positions (Figure 1), while the second version makes use of matplotlib (Figure 2), using elaborated illustrations to make the work clearer. The three-body problem, the initial positions, velocities and masses of three stars are taken to solve for their subsequent motion according to Newton's three laws of motion and law of universal gravitation

STAR\_1 POSTION: X: 602.6255095661821 Y: 301.2000001037916 Z: 200.48724537259622

STAR\_2 POSTION: X: 801.1997058408364 Y: 301.2002853105119 Z: 101.20057504534981

STAR\_3 POSTION: X: 999.774397270562 Y: 301.2003209634784 Z: 1.9132828099366446

Figure 1. The initial code for data showing

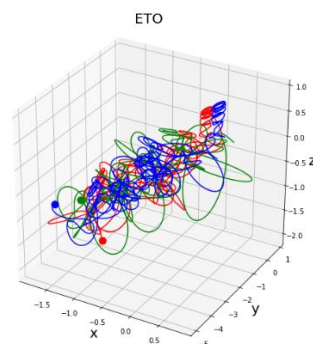


Figure 2. A completely random three-body simulation[1]

## 2. Chaotic system behind the three-body problem

### 2.1 The restrictive Conditions of Three-body Chaotic System [2]

The masses of three gravitationally interacting bodies are expressed in terms of  $m_1, m_2, m_3$ . The position and the velocity of a star are expressed in vector  $r_1 = (x_1, y_1, z_1)$  and the velocity  $v_1 = (v_{x1}, v_{y1}, v_{z1})$  with measurements in three-dimensional space.  $\lambda$  stands for the array of the parameters of a star, which is expressed as:

$$\lambda = (r_n, v_n, m_n) \quad (1)$$

According to the conservation of momentum, angular momentum, and energy, the energy, momentum, and angular momentum in the system can be expressed, with the use of Newtonian equations[3]:

$$\text{Total energy of the system} = \sum E = G \frac{m_1 m_2}{D_{12}} + G \frac{m_1 m_3}{D_{13}} + G \frac{m_2 m_3}{D_{23}} + \frac{1}{2} \sum_{n=1}^3 m_n v_n^2 \quad (2)$$

$$\text{Total momentum of the system} = \sum p = \sum_{n=1}^3 m_n v_n \quad (3)$$

$$\text{Total angular momentum of the system} = \sum l = \sum_{n=1}^3 m_n v_n (r_n - \frac{\sum_{n=1}^3 m_n r_n}{\sum_{n=1}^3 m_n}) \quad (4)$$

Thus,

$$2(E_n - (G \frac{m_n m_{n'}}{D_{nn'}} + G \frac{m_n m_{n''}}{D_{nn''}})) = G \frac{m_n(m_{n'} + m_{n''})}{r_n - \frac{m_{n'} r_{n'} + m_{n''} r_{n''}}{r_{n'} + r_{n''}}} \quad (5)$$

$$r_n = G \frac{m_n(m_{n'} + m_{n''})}{2(E_n - (G \frac{m_n m_{n'}}{D_{nn'}} + G \frac{m_n m_{n''}}{D_{nn''}}))} + \frac{m_{n'} r_{n'} + m_{n''} r_{n''}}{r_{n'} + r_{n''}} \quad (6)$$

Instantaneous values for each parameter could be plugged into formula (5) and (6) to calculate the position of a certain star. In the simulation, the nondimensionalizing method is used to put the simulation's data to be more mathematic and readable, which means that the data given in the simulation is not supposed to be accurate, but the proportional relation will be clear and useful for expressing our meaning.

Since the trajectories of special solutions in three-dimensional space are much less than those in two-dimensional[4] space, the simulation of the restricted three-body problem is operated in two-dimensional space. All initial parameters needed are plugged in to see whether the three stars could continue their motions as chaotic three-body system.

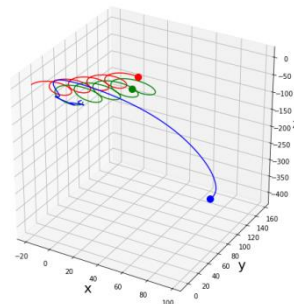


Figure 3. Systems Simulated (ending up with binary system)

However, almost all the simulated systems ended up being a binary system formed by two greater stars, while the smallest star being left away. The probability of ending up binary system is 93.4%, summarized by Anosova, Z. P (Anosova, Z. P, 1990) [5], which deviates our aim to find the special solutions to the three body problems.

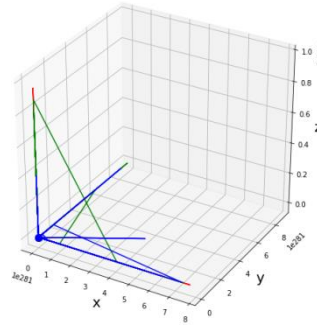


Figure 4. Computer errors because of the collision

Other than systems ending up with forming binary system, there are a few parts of the system turning into collision. In this case, the distance of those stars is infinitely small as stars are assumed to be mass point.

Assume that the  $D_{123}$  is the star 1's distance to the center of mass (CM) of other two stars, the  $D_{12}$  represents the distance between star 1 and 2. According to the formula

$$\frac{v_{12}^2}{D_{123}^2} = \frac{Gm_2}{D_{12}^2} + \frac{Gm_3}{D_{13}^2} \quad (7)$$

Two of three stars will have infinitely small distance in between during collision, so there must be a bug in calculation to run the code.



Figure 5. the intension to form the binary system

According to Figure 5, even though the initial values are set for each parameter to let the three stars collide toward each other's center of mass, they end up forming a binary system, because the approximation of parameters is plugged in, instead of the exact value of square root of 3. Furthermore, by comparing the probability of colliding with other stars with the probability to form the binary system, this simulation shows collision is infrequent. In some cases, it seems that a perfect chaotic system come into being. However, even if the three stars form a chaotic system for a period of time, all three-body systems that does not exhibit special patterns will eventually end up two possible outcomes above (binary system or collision). In the simulation shown above, the system turns out to be a binary system and an isolated single star. Therefore, considering chaotic system as a three-body initial system without deduction would benefit the study.

According to

$$\text{Degree of Freedom} = DF = 3n - 2P_L - P_h \quad (8)$$

where  $n$  stands for number of bodies in the system;  $P_L$  stands for lower pairs,  $P_h$  stands for higher pairs.

And the total energy, momentum, and angular momentum are

$$\sum E = G \frac{m_1 m_2}{D_{12}} + G \frac{m_1 m_3}{D_{13}} + G \frac{m_2 m_3}{D_{23}} + \frac{1}{2} \sum_{n=1}^3 m_n v_n^2 \quad (9)$$

$$\sum p = \sum_{n=1}^3 m_n v_n \quad (10)$$

$$\sum l = \sum_{n=1}^3 m_n v_n (r_n - \frac{\sum_{n=1}^3 m_n r_n}{\sum_{n=1}^3 m_n}) \quad (11)$$

Degree of freedom (DOF) determines the duration of chaos and the possibility of the existence of a particular solution in a chaotic system. From the formula, it can be shown that the degree of freedom (DOF) of unrestricted three-body system can be changed from  $3 \times 2 \times 3$  to  $2 \times 2 \times 3$ . By cutting down the degree of freedom of it, the system runs as a restricted two-dimensional three-body pattern.

The DOF of the n-body system linearly increases by  $6n$ . So, for the n-body problem, the probability of de-chaotic systems will be greater. In fact, the research's aim is not to find a de-chaotic three-body system (binary systems or collision systems), but a particular solution based on long-term chaos.

For n-body, the coordinate and velocity vectors are introduced in three-dimensional space.

$$r_n = (x_n, y_n, z_n) \quad (12)$$

And

$$v_n = (x'_n, y'_n, z'_n) \quad (13)$$

Thus, a summary of the n-body motion could be conducted by using two vectors for one star and the system

$$\lambda = (r_n, v_n, m_n) \quad (14)$$

$$C = (\Sigma E, \Sigma p, \Sigma L) \quad (15)$$

Even in the two-dimensional plane, the final three-body random system can only lead to two distinct results: either a collision, or a binary system. According to statistics, although the chaotic state of the two-dimensional restricted three-body problem occurs much later than that of the three-dimensional unrestricted three-body problem, the data tells us that seeking the stable solution of the two-dimensional plane is still the only feasible measure. In the simulation of some systems, the two-dimensional constraint plane is used for the experiment, and the special three-body permanent stable solution is explored in the two-dimensional constraint plane.

## 2.2 Chaotic systems of One Simple Restricted Three-body Solution (Equilateral)

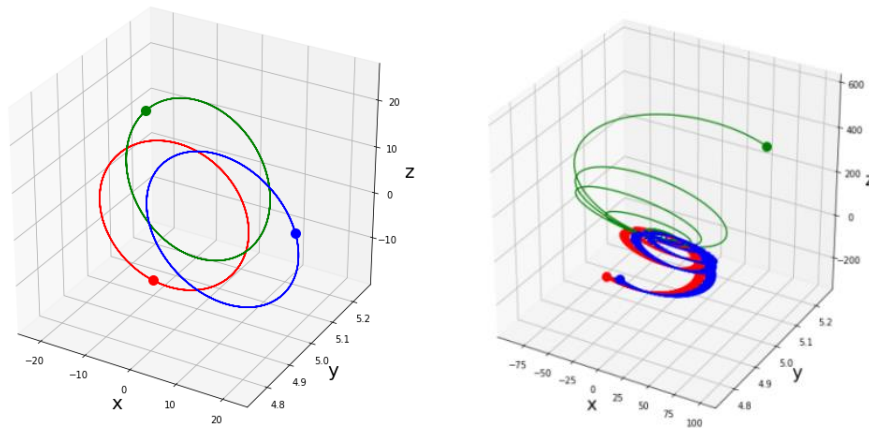


Figure 6. Stable System (initial) Figure 7. Binary System (Ultimate)

Figure 6 and 7 come from same initial parameter. The running time in-between is two orders of magnitude different from each other. The reason of the seemingly stable equilateral triangle three-body system eventually turning into binary is that when the initial quantity is inputted, the approximation of the square root of 3 to the 9<sup>th</sup> place after the decimal point was used. Even though the numbers are very accurate, the equilateral triangle system still appears chaos. This shows that permanent stable systems, such as equilateral triangle systems, which require strict initial parameters, are almost impossible to exist in reality.

```
#blue star↵
m3=70↵
r3=[20,5,-10]↵
v3=[-2,0,-3.464101615]↵
```

Figure 8. Example of the Initial Parameters  
(Approximation)

```
v1=[0,0,0] ↵
v2=[0,-1,0]↵
v3=[-0.5*gensan,-0.5,0]
```

Figure 9. Example of the Initial Parameters  
(Precise Value)

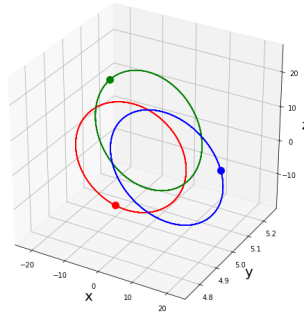


Figure 10. Equilateral Three-body Systems Solution

As shown in Figure 13, the estimated value with the root 3 is replaced, and a permanent stable three body system appears. Also, from this model, the result shows the similarity between the chaotic three-body problem and the Lorenz system (Edward Norton Lorenz, 1963) [6].

According to the Lorenz's differential equation,

$$\frac{dx}{dt} = \sigma(y - x) \quad (16)$$

$$\frac{dy}{dt} = x(\rho - x) - y \quad (17)$$

$$\frac{dz}{dt} = xy - \beta z \quad (18)$$

There are 3 variables, which can be seen in the space, with  $DOF=3$ . Also, it could be assumed that the three variables are the three initial parameters. So, initials  $x=10$  and  $x=10.001$  (leave all other variables the same) are plugged into the two simulations to demonstrate the chaotic system. The time  $t$  was also altered to see clearly what parameter is changing. The simulation of Lorenz system is presented below in Figure 14, and 15:

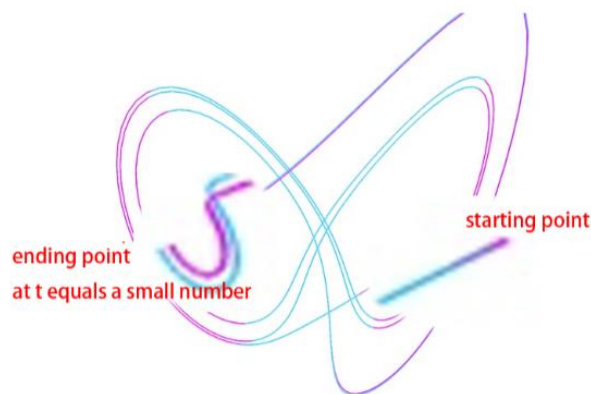


Figure 11. The Simulated Lorenz System (initial)

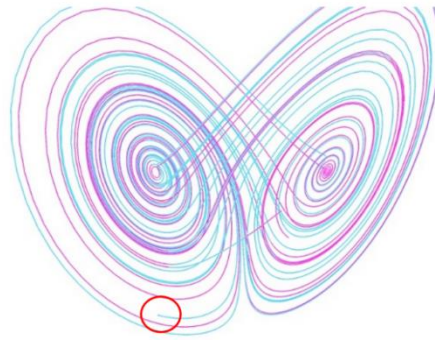


Figure 12. The Simulated Lorenz System (final)

Thus, it can be shown that in Lorenz system, although it has only 3 DOF, which is 9 DOF lower than the restricted two-dimensional three-body motions, while there is only a slight difference between the initial parameters. The chaotic systems become completely chaotic eventually.

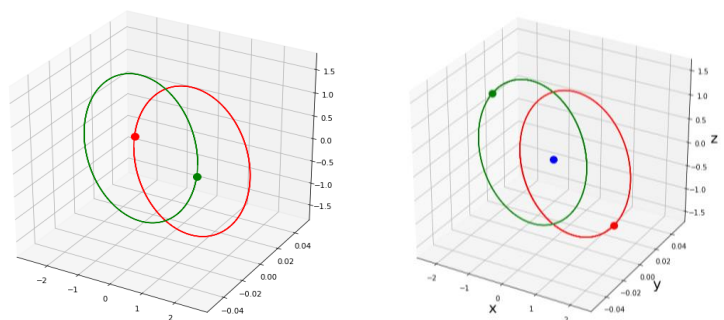
Let us look at the three body systems. Because the two-dimensional restricted three-body systems have 9 DOF greater than the Lorenz system, the chaotic must appear.

### 3. Lagrangian Points Analysis[7]

This part of analysis consists of stationary and dynamic helical situation simulation, Euler's solution, and Lagrangian points (L4, L5). With the help of helical situation, the motion of the whole system can be calculated while central star is moving and simulate the dynamical stability in helical situation, which is a more sophisticated analysis that cannot be done by Lagrangian points (L4, L5). In fact, Helical situation is a special case of Euler's solution, since Euler's solution is L1, L2, and L3 of Lagrangian points. The aim of distinguishing them as Euler's solution and Lagrangian points (L4, L5) is for making contrasts. Since the relative position of L4 and L5 is in two-dimension rather than one-dimension, and Coriolis force is also valuable to the study of three-body system stability.

#### 3.1 The Stationary Helical Situation

According to Figure 13, a greater mass of a central object will create more gravity. The orbital coordinates of the other two celestial bodies prove our assumption. According to the universal gravitation equation, the size of gravity will affect the radius of the orbits. However, according to Kepler's first law, the surrounding objects (in a three-body system, although the object is uncertain, it can be assumed that the other two stars are like a single star within a certain range) must be in one focus of the ellipse[8], so the situation in the following simulation should be the case. According to the simulated coordinates, it can be shown that with the increase of  $m_3$ , the orbit radius of the other two celestial bodies becomes smaller and smaller, but their orbits do not shrink in an equal proportion, but shrink towards the direction of  $m_3$ . Therefore, the phenomenon of seemingly orbit exchange (which is shown below) will appear. The fact is that they are zooming in and out of one focus, and their orbits' position is essentially uncha



a. No Third Mass

$$b. m_3 = \frac{m_1 + m_2}{100}$$



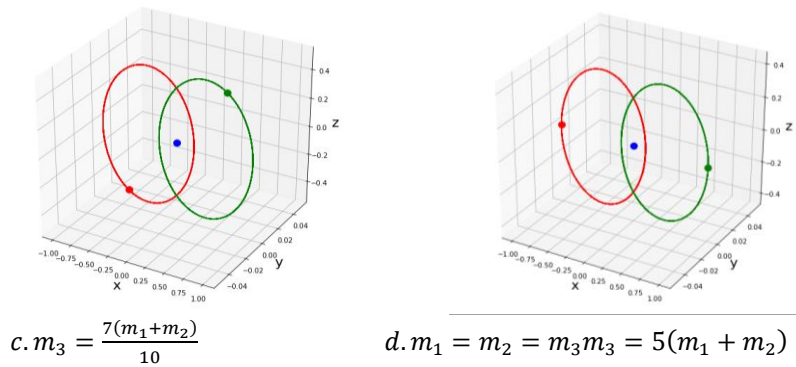


Figure 13. Three-body system (With Increasing 3rd Mass)

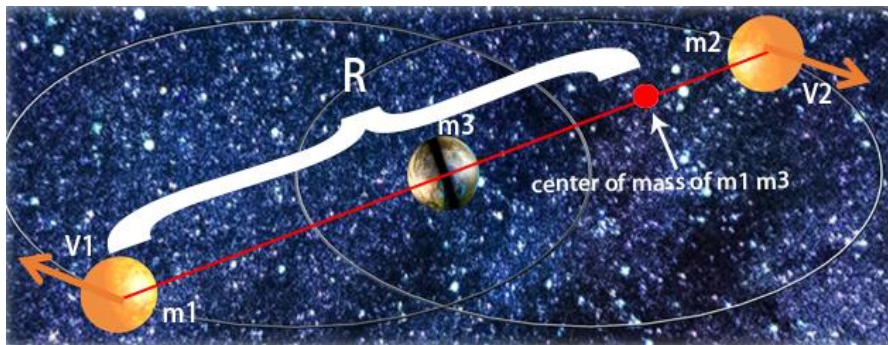


Figure 14. The illustration of helical situation

In Figure 14, the three stars are in the same line, so a summarized formula to calculate the relationship between the mass of the central star ( $m_3$ ) and the radius of the other two stars ( $r_1$ ,  $r_2$ ) is obtained. In fact, according to Figure 14,  $m_2$  and  $m_3$  could be simplified as one star in their center of mass, which will form the binary system with  $m_1$ .

$$F_G = G \frac{m_1 (m_2 + m_3)}{(R - \frac{m_1 r_1 + m_2 r_2}{r_1 + r_2})^2} \quad (19)$$

After the calculation and simulation, the work shows that the helical situation is similar to the Euler's Solution. In the helical situation, because the central celestial body is a planet, which is supposed to have less mass and the position of the planet is also at a special point, its influence to the system is not as important as the center star of Euler's solution. The  $m_3$  does not have an eclipse orbit for itself, so the center of mass of the three stars is on the planet itself. For the Euler's solution, integrals could be done of the two stars that have smaller mass to let those two stars to be seen as one star in the helical situation.

### 3.2 The Dynamical Helical Situation

To expand the analysis to the dynamical helical situation in three-dimensional space and find out whether this helical situation allows us to have a permanently stable solution other than three-body systems in two-dimensional restricted system.

By observing the system directly from the horizontal plane, the assumption that  $m_1$  will form binary system with  $m_2$  and  $m_3$  will become complex since the system goes dynamic, because the influence from only one initial speed from  $m_3$  to all of the stars ( $m_3$  to  $m_2$ , to the center of mass of  $m_2$  and  $m_3$  and thus to  $m_1$ ;  $m_3$  to  $m_1$ , to the center of mass of  $m_1$  and  $m_3$  and thus to  $m_2$ ) should be taken into account. Based the previous analysis, since the degree of freedom is increased by 6 (12 to 18), there must be a more complex question. Figure 20 shows that the influence of initial velocity  $v$  to two masses ( $m_3$  to  $m_2$ , and the center of mass of  $m_2$  and  $m_3$  to  $m_1$ ).

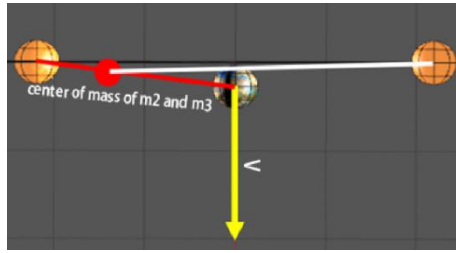


Figure 15. Horizontal View of the Dynamic Helical Situation

Although the velocity and the attraction by the central object on the other two objects is figured out and it can be shown that the dynamical helical system is not a permanent stable system, the problem is difficult to be analyzed by mathematical methods. So, the simulation is used to show that the system will finally collapse, and the simulated outcomes proved our thought. As the figure 20 shown, the dynamical helical solution ends up chaotic. Thus, this work shows that the Lagrangian points are limited in the restricted two-dimensional three-body problems.

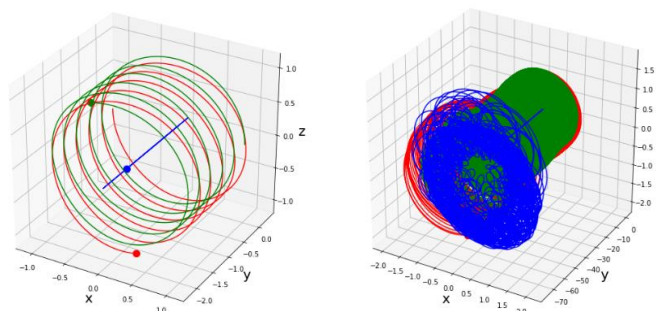


Figure 16. Dynamic Helical Situation ( $m_3=11$ ,  $v=1$ )

As shown in Figure 16, it can be shown that the helical situation could not be a stable solution to three-dimensional three-body problem because the system will finally collapse because the  $m_3$  gives a unbalanced acceleration in y- axis.

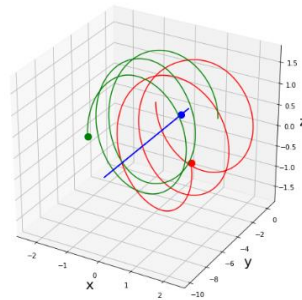


Figure 17. Chaotic System ( $m_3=11$ ,  $v=2$ )

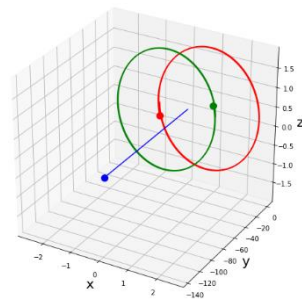


Figure 18.  $m_3$  expelled ( $m_3=11$ ,  $v=5$ )



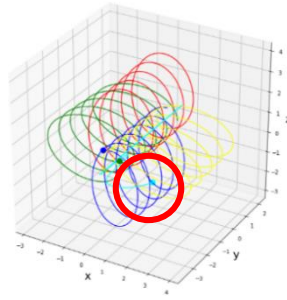


Figure 19. Five-body Helical Situation (Dynamic)

As shown in Figure 17, when  $m_3=11$ ,  $v=2$ , The third masses control the system loosely, so it will become chaotic system. In Figure 18, when  $m_3=11$ ,  $v=5$ ,  $m_3$  will leave the system because the speed of the center.

Other than analysis for the three-body system, the research attempts to figure out the stability of the helical solution in n-body systems. In Figure 19, dynamical five-body helical situation is simulated.

### 3.3 Euler's Solution[11] (Lagrangian point L1, L2 and L3)

A clarification should be made before the analysis of Euler's solution. Consider that L1, L2 and L3 are more likely to contain the stars while the L4 and L5 are expected to form star-planet system. And for recognizing, Euler's solution is used to represent the Lagrangian point L1, L2 and L3.

Compared with Lagrangian point L4 and L5, the Euler's solution is not suitable in the initial condition.  $m_2$  must orbit exactly around the center of mass that satisfy the following equation:

$$\frac{v_2^2}{r_2} = \frac{Gm_1}{D_{12}^2} + \frac{Gm_3}{D_{13}^2} \quad (20)$$

Because all the parameters (except the mass of the stars) are vectors, this formula could be used on all of the stars.

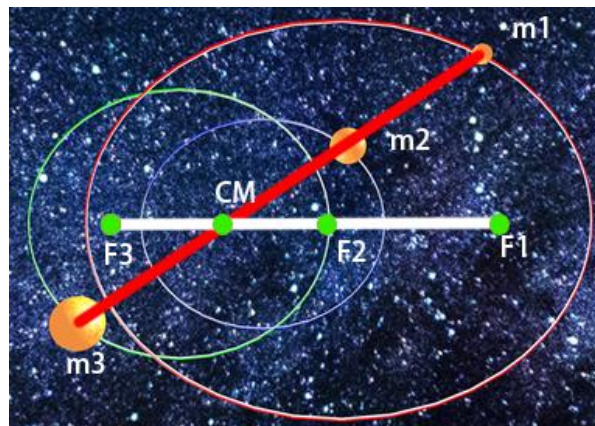


Figure 20. Euler Colinear Situation ( $m_1:m_2:m_3 = 1:2:3$ )

The Euler's solution is supposed to have different masses, which is shown above. In this model, all the stars are on the same line. Firstly define the CM as the origin of a coordinate system, and apply vector of position and velocity ( $r_1 = (x_1, y_1, z_1)$ ,  $v_1 = (v_{x1}, v_{y1}, v_{z1})$ ),  $m_1, m_2, m_3$  and  $D_{12}$  to indicate the initial parameters.

$$\frac{v_n^2}{r_n} = \frac{Gm_n}{D_{nn}^2} + \frac{Gm_n}{D_{nn}^2} \quad (21)$$

Because they are collinear,

$$r_n \omega^2 = \frac{Gm_n}{D_{nn}^2} + \frac{Gm_n}{D_{nn}^2} \quad (22)$$

From using the vector, it could be changed it into another formula

$$v_n = \frac{d(\frac{Gm_n}{D_{nn}^2\omega^2} + \frac{Gm_n}{D_{nn}^2\omega^2})}{dt} \quad (23)$$

By using the conservation of momentum

$$\frac{d(\frac{Gm_2}{D_{12}^2\omega^2} + \frac{Gm_3}{D_{13}^2\omega^2})}{dt} + 2\frac{d(\frac{Gm_1}{D_{12}^2\omega^2} + \frac{Gm_3}{D_{23}^2\omega^2})}{dt} + 3\frac{d(\frac{Gm_1}{D_{13}^2\omega^2} + \frac{Gm_2}{D_{23}^2\omega^2})}{dt} = 0 \quad (24)$$

The velocity can also be used to calculate the total energy if the initial parameters are known:

$$\sum E = G\frac{m_1m_2}{D_{12}} + G\frac{m_1m_3}{D_{13}} + G\frac{m_2m_3}{D_{23}} + \frac{1}{2}\sum_{n=1}^3 m_n v_n^2 \quad (25)$$

### 3.4 Lagrange's Solution (L4/L5)

#### 3.4.1 Analysis of L4 and L5

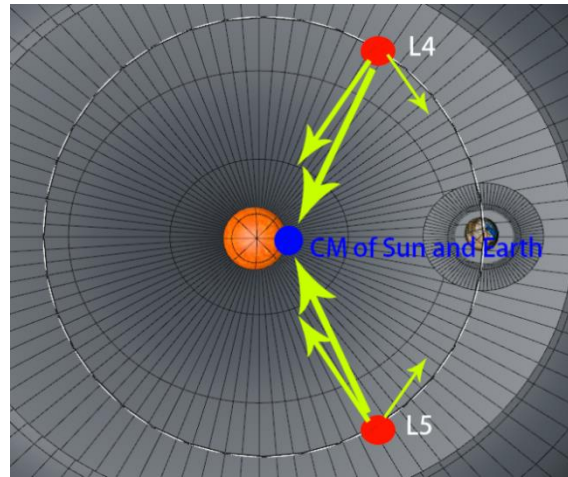


Figure 21. L4 and L5 (in Gravitational Field)

For the motion of L4 and L5, different from Euler solution (L1, L2 and L3) and the helical solution, the stars are in a two-dimensional surface instead of a one-dimensional line, which will certainly increase the degree of freedom and add more component vectors to the system. The L4 and L5 must satisfy an assumption that the masses on these point L4 and L5 are ignorable. According to Figure 21, the orbiting center of the bodies at L4 and L5 is the center of mass of sun-earth system, and for stars and planets, the star mass should be more than 24.96 times[12] greater than the planet to have the L4 and L5.

Unlike Euler solution, Lagrangian points L4 and L5 do not require rigorous precision, because L4 and L5 are not points but a certain area of motion, due to Coriolis Force, a kind of inertial force exerting on the bodies at L4 and L5. Thus, they can re-obtain the previous orbiting velocity through orbital compression when they are about to leave Lagrangian points.

Use Coriolis force to analyze the stability of the bodies at L4 and L5. Assume the mass of the sun is  $m_1$ , and the mass of the earth is  $m_2$ . The mass at L4 or L5 is  $m_3$ . According to:

$$F - m\frac{v^2}{r} = 2mv'\omega + mr\omega^2 \quad (26)$$

Assume  $v'$  is the velocity relative to the rotating reference frame. Because the system of L4, L5, and the sun are equilateral triangle, assume  $r_1 = r_2 = r_3 = R$ , the expression of Coriolis force can be derived:

$$F = 2m_3v'\omega$$

At L4 and L5,  $m_2$  and  $m_3$  have the same angular velocity, thus:

$$\frac{dv}{dt} = \left(2 \sqrt{\frac{Gm_1}{R^3}}\right) \frac{dR}{dt} \quad (27)$$

Therefore, along with  $m_3$  leaving Lagrangian point, Coriolis force will offer  $m_3$  a tangential acceleration perpendicular to the orbit radius, which compresses the orbit of  $m_3$  guaranteeing  $m_3$  will not leave Lagrangian point.

### 3.4.2 The Chaotic System of Lagrange's Solution (L4/L5)

In addition, the Lagrange's Solution is simulated. From those figures, it can be assumed that the red point is the main star, the green point is the planet and the blue point is the celestial body that has infinitely small mass.

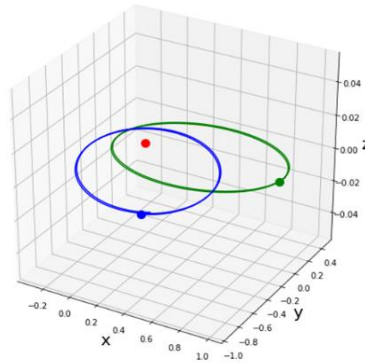


Figure 22. Stable System

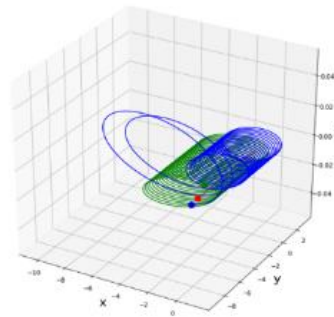


Figure 23. Unstable Lagrange system that has 2 times greater initial speed

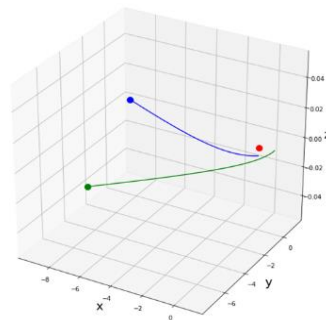


Figure 24. Unstable Lagrange system that has 2.25 times greater initial speed

These figures show cases of the unstable Lagrange solution that changes over time (difference timespan), which shows a pattern that initially stable but finally collapse (they all have TWICE speed compared with the stable system). Larger difference of velocity of three-body is shown in this Lagrange's Solution because the speed is a little greater. (the speed is only 2.25 times higher than the stable solution)

In conclusion, a slight influence on speed would lead to a great change in Lagrange's Solution. And as the time goes by, those system seems to be stable became chaotic finally.

#### 4. Three stars solution

In this part, the solutions that contain three stars that have similar masses are simulated and analyzed.

##### 4.1 Figure-eight Solution[9]

The model and stability of the figure-eight configuration are proposed by Chenciner and Montgomery [2001]. The complex motion of figure-eight movements can also be broken down into two simple situations which are Euler collinear situations and isosceles triangle situations as shown below.

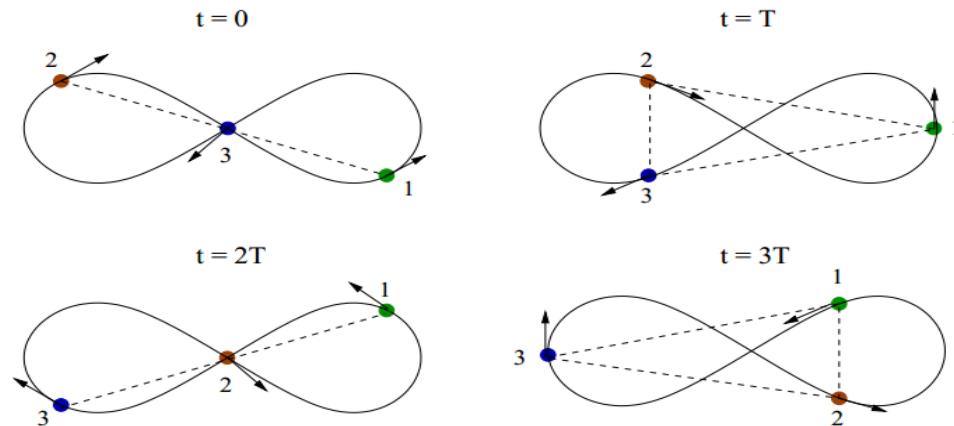


Figure 25. Figure-eight solution [10]

To explore the stability of the figure-eight solution, it is necessary to consider the initial phase of three masses. It can be assumed that all three particles have the same mass. If three particles are placed randomly on the eight-shaped orbit, the three-body system will be a chaos. Therefore, it is applicable to consider the system as a two-body system and put the one particle on each side to balance them. The next step is to place the third particles to satisfy the following equations.

The whole system can be represented as

$$x(t) + x\left(t + \frac{1}{3}T_0\right) + x\left(t + \frac{2}{3}T_0\right) = 0 \quad (28)$$

$$y(t) + y\left(t + \frac{1}{3}T_0\right) + y\left(t + \frac{2}{3}T_0\right) = 0 \quad (29)$$

These equations not only prove the great symmetry in the figure-eight movements in special cases but also show the prerequisite of the eight-figure solution.

One of the most notable features in the figure-eight solution different from the previous solution is the feature of the period. For convenience, define the eight-shaped planar position function  $x(0)=(0,0)$  for  $\forall x \in \mathbb{C}$ , and define the intersecting point in the middle as the origin point. The whole period is defined as  $T$ , and the small interval is defined as  $T_0$ . Therefore,  $12T_0=T$ . The intervals which travel between the collinear situation and isosceles situation are equal as proved by Chenciner and Montgomery [2001]. It always takes  $T_0$  to travel from the collinear situation and isosceles situation. After reaching the position of isosceles situation, three masses also take  $T_0$  to go back to the collinear situation. Assuming that all masses are equal, some interesting conclusions toward the period can be made. Their initial time can set as  $0, \frac{1}{3}T_0, \frac{2}{3}T_0$ , in order to sustain their periodic motion. No matter when they travel the sum of the x-coordinate and y-coordinate is the same which equals the position of the origin point. That is

$$x(t) = \left(x(t), x\left(t + \frac{1}{3}T_0\right), x\left(t + \frac{2}{3}T_0\right)\right) \quad (30)$$

$$y(t) = \left(y(t), y\left(t + \frac{1}{3}T_0\right), y\left(t + \frac{2}{3}T_0\right)\right) \quad (31)$$

#### 4.2 Chaotic System in Figure-eight Solution

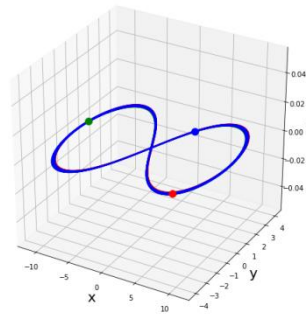


Figure 26: Stable simulated Figure-eight Model

In this seemingly stable simulation in Figure 26, the initial parameters are  $r_1 = [10, -2, 0]$ ,  $r_2 = [-10, 2, 0]$ ,  $r_3 = [0, 0, 0]$ ;  $m_1 = m_2 = m_3 = 10$ ;  $v_1 = v_2 = [1.7, 1.7, 0]$ ,  $v_3 = [-3.4, -3.4, 0]$ ; and the time span is 2000, which is obviously enough for proof of the stability. After that, some of the initial parameters are changed to see if there is any difference.

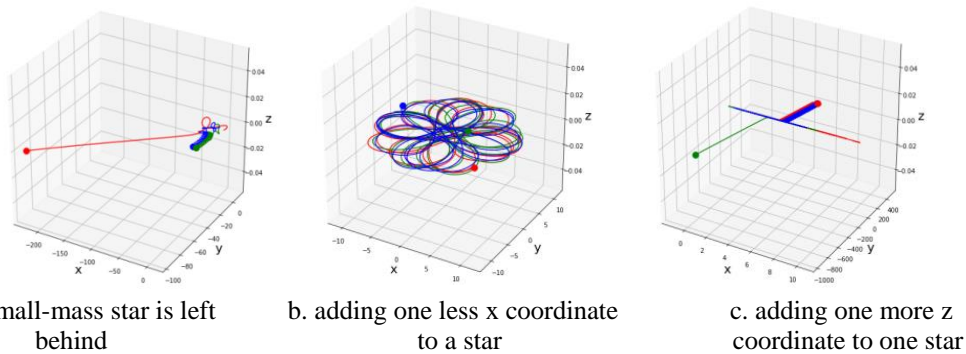


Figure 27. Four Chaotic Systems of Figure-eight Solution

The left figure is the result of one small-mass star, which is left behind the other two stars. Those two stars finally form a stable binary system. The middle figure is the result of adding one less x coordinate to one star, and the right figure is the result of adding one more z coordinate to one star. Both of the systems are chaotic and they will turn into binary system or hit and collapse. This work also finds that change of z coordinate will be more likely to ruin the three-body system, which is consistent with the finding of DOF mentioned before.

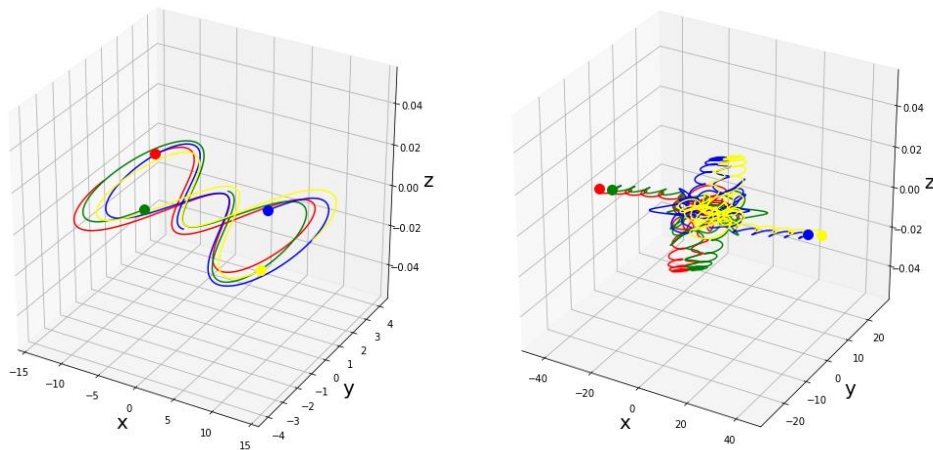


Figure 28. The System of Four-body Figure-eight Solution

The left figure shows a seemingly stable system, which will still collapse. It is realized that the four-body figure-eight solution is difficult to simulate (or to find the initial conditions of the four stars).

The result that the figure-eight model should also be treated with numerical accuracy. According to



the deduction, the parameters of the four-body figure eight movement should be more precise than those of the three-body figure eight movement, which is why the image is inaccurate.

#### 4.3 Stable System with a seemingly Chaotic System and a Single Star

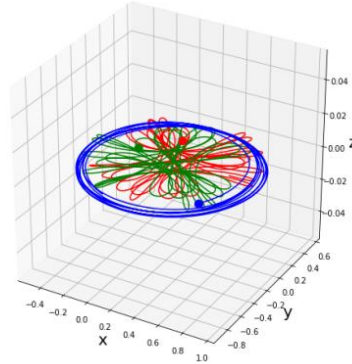


Figure 29. Stable System with 2 Seemingly Chaotic Stars

Figure 29 exhibits a system in which two stars are regarded as a whole and a third star is in a circular orbit. Integrals could be applied to analyze the system. (assume blue star is  $m_3$ ,  $F_G$  is the gravitational force and  $T$  is the period)

$$\frac{\sum_{n=1}^2 m_n r_n}{\sum_{n=1}^2 m_n} (\text{average}) = \frac{\int_{t_1}^{t_2} (r_1 + r_2) dt}{t_2 - t_1} \quad (32)$$

$$F_G = G \frac{m_3 (m_1 + m_2)}{(r_3 - \frac{\int_{t_1}^{t_2} (r_1 + r_2) dt}{t_2 - t_1})^2} \quad (33)$$

$$T = \sqrt{\frac{4\pi r_3 m (r_3 - \frac{\int_{t_1}^{t_2} (r_1 + r_2) dt}{t_2 - t_1})^2}{m_3 (m_1 + m_2)}} \quad (34)$$

Thus, the outcomes (parameters) of the computer simulation can be used to calculate the period of a stable system with a seemingly chaotic star system and a single star. Because accurate values can not be obtained, this system has the limitation that it can only be regarded as a solution within a certain time.

#### 4.4 The Stable Rotation System

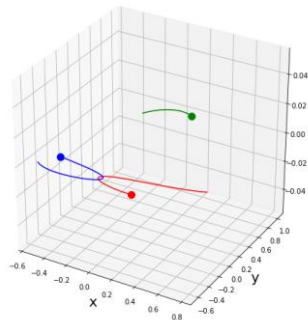


Figure 30. Timespan = 1

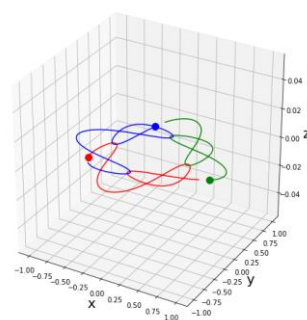


Figure 31. Timespan = 5.5

In Figure 30, the system is not significantly different from other random trisomy chaotic systems in the initial state. In Figure 31, it can be shown that the three-body regular motion pattern of the system comes from the binary transformation trend of the three-body system.



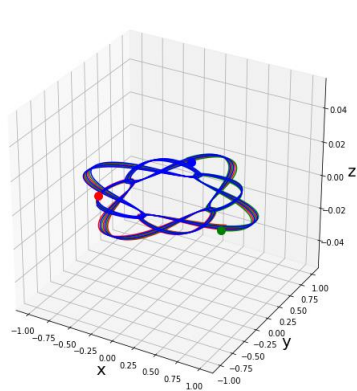


Figure 32. Timespan=40

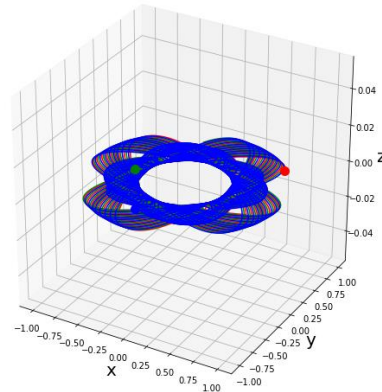


Figure 33. Timespan=500

There are more regular motion patterns other than that. However, from observing the motion state of the above two pictures, it seems that there is still an overall movement trend of the three-body system.

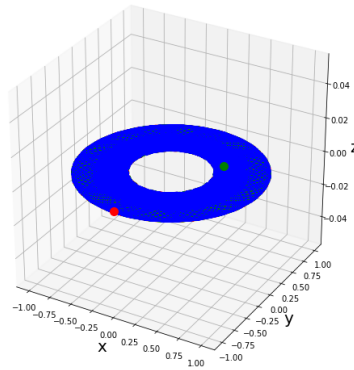


Figure 34. Huge Timespan

In the end, as expected, the three-body motion forms a disc. Because there is no exact numerical value, this system can only be regarded as a solution in a certain time period. The relationship between the radius of the disc and the initial speed is also a main concern of our research.

## 5. Conclusion

In this paper, the reason behind three-body system's chaoticity has been elaborated. By introducing the concepts in mechanics degrees of freedom, the work shows the real factors behind the chaoticity. Also, the result of a real unrestricted three-body system will end up binary system or a collision in the process of evolution from three-body system to binary system has been shown in numerous simulations. So, by reducing the system DOF to form two-dimensional restricted three-body systems, our simulations could help to find special cases in two-dimensional restricted three-body problems

Apart from that, analysis with the most classical special cases of two-dimensional restricted three-body problems, the Lagrangian points are analyzed. The similarity and difference between stationary helical systems, dynamic helical systems, Euler's solution and Lagrangian points for L4 and L5 have been shown in the work. In fact, all of the Lagrangian points could be integrated and simplified as helical solution. Also, this work shows that any difference on the z-value will ruin the stability of the systems because it adds more DOF to the systems.

Furthermore, this paper presents some two-dimensional special solutions to three-body problem. They are figure eight solution, the stable system with a seemingly chaotic system and a single star and the stable rotation system. The mathematical analysis to calculate the period of them and the computer simulation to show their stability have been displayed clearly in the paper.

All in all, this paper gives innovative analysis to the factor that causes the chaoticity of three-body problems and new definition to the chaotic three-body systems. Apart from that, New computer and

mathematical analysis to the two-dimensional special restricted three-body cases are given. From this work, future researchers will be able to better analyze the chaotic systems behind the three-body problems by computer simulation and integrals. In the future work, statistical tools will be in need to calculate the probability of the motion pattern of random three-body systems. Also, the mathematical way to calculate the degree of chaotic is expected to be found.

## References

- [1] Anosova, Z. P., *Computer simulations in the general three-body problem - The theoretical bases of the studies, Celestial Mechanics and Dynamical Astronomy (ISSN 0923-2958). [1990]. vol. 48, no. 4, 1990, p. 357-373.*
- [2] Z.E. Musielak and B. Quarles. *The three-body problem, Reports on Progress in Physics arXiv:1508.02312v1 [astro-ph.EP] 10 Aug 2015*
- [3] Jules Henri Poincaré *New Methods of Celestial Mechanics*[1892–1899]
- [4] Szebehely V., *Theory of orbits: the restricted three body problem, Academic Press. [1967]. p. 126-230*
- [5] Anosova, Z. P., *Computer simulations in the general three-body problem - The theoretical bases of the studies, Celestial Mechanics and Dynamical Astronomy (ISSN 0923-2958), [1990]. vol. 48, no. 4, 1990, p. 357-373.*
- [6] Edward Norton Lorenz, *Deterministic Nonperiodic Flow, Journal of the Atmospheric Sciences. [1963]. Vol.20, p.130-141.*
- [7] Lagrange J L., *Essai sur le probleme des trois orps -uvres, [1772]. vol. 6 p 273*
- [8] Kei Yamada and Hideki Asada, *20th workshop on General Relativity and Gravitation in Japan(JGRG20). [2001]. p. 440-443.*
- [9] C. Simó, *Dynamical properties of the figure eight solution of the three-body problem. Preprint. (Departament de Matematica `Aplicada i Analisi. Universitat de Barcelona). Mexico oct.2003. vol. 49, no.5*
- [10] A. Chenciner and R. Montgomery, *A remarkable periodic solution of the three-body problem in the case of equal masses, Ann. of Math., November. [2000]. vol. 152, p. 881-901*
- [11] Euler; Leonhard, *"De motu rectilineo trium corporum se mutuo attrahentium" (1767). Euler Archive - All Works. 327.*
- [12] Matthew Beckler. *Behavior of Satellite Objects in the Earth-Moon Lagrange Points. arXiv:1912.01894v1 [astro-ph.EP] 4 Dec 2019.*